

# Recent results from Belle

P. Krokovny

*Budker Institute of Nuclear Physics, Novosibirsk, Russia*

**Abstract.** New results on hadron physics from the Belle experiment are presented.

## INTRODUCTION

These results are obtained using various data samples from  $80 \text{ fb}^{-1}$  to  $150 \text{ fb}^{-1}$  taken with the Belle detector [1]. We identify  $B$  candidates by two kinematic variables: the energy difference,  $\Delta E = (\sum_i E_i) - E_b$ , and the beam constrained mass,  $M_{bc} = \sqrt{E_b^2 - (\sum_i \vec{p}_i)^2}$ , where  $E_b = \sqrt{s}/2$  is the beam energy and  $\vec{p}_i$  and  $E_i$  are the momenta and energies of the decay products of the  $B$  meson in the CM frame. The inclusion of charge conjugate modes is implicit throughout this report.

## OBSERVATION OF $0^+$ AND $1^+$ BROAD $C\bar{U}$ STATES

A study of charmed meson production in  $B$  decays provides an opportunity to test predictions of Heavy Quark Effective Theory (HQET) and QCD sum rules.  $B$  decays to  $D^{(*)}\pi$  final states are its dominant hadronic decay modes and are measured quite well [2]. The large data sample accumulated in the Belle experiment allows to study production of  $D$  meson excited states.  $D^{**}$ s are P-wave excitations of quark-antiquark systems that contain one charmed and one light ( $u, d$ ) quark.

$B \rightarrow D^{**}\pi$  decays have been studied using the  $D^+\pi^-\pi^-$  and  $D^{*+}\pi^-\pi^-$  final states [3].

Figure 1 shows the  $\Delta E$  distributions for the  $B^- \rightarrow D^+\pi^-\pi^-$  and  $B^- \rightarrow D^{*+}\pi^-\pi^-$  candidates. The following branching fractions are measured:  $\mathcal{B}(B^- \rightarrow D^+\pi^-\pi^-) = (1.02 \pm 0.04 \pm 0.15) \times 10^{-3}$  and  $\mathcal{B}(B^- \rightarrow D^{*+}\pi^-\pi^-) = (1.25 \pm 0.08 \pm 0.22) \times 10^{-3}$ , without any assumption about the intermediate final states.

To study the dynamics of  $B \rightarrow D^{(*)}\pi\pi$  decays, analyses of the Dalitz plots are performed. The description of the Dalitz plot  $D^+\pi^-\pi^-$  includes amplitudes of the known  $D_2^{*0}\pi^-$  mode, possible contributions of the processes with virtual  $D^{*0}\pi^-$  and  $B^{*0}\pi^-$  production and an intermediate  $D^+\pi^-$  broad resonance structure with free mass and width. Figure 2(a) shows the  $D^+\pi^-$  invariant mass distribution together with the resulting fit. A clear signal of the broad resonance with  $J^P = 0^+$  is observed which can be identify as the scalar  $D_0^{*0}$  state. The results of the mass, width and branching fraction products are

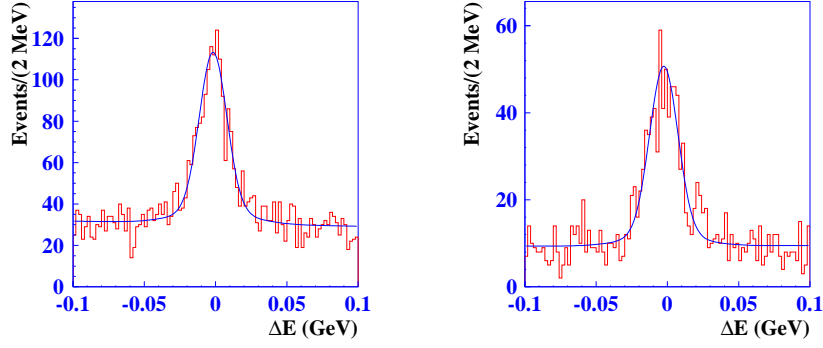


FIGURE 1.  $\Delta E$  distributions for the  $B^- \rightarrow D^+ \pi^- \pi^-$  (left) and  $B^- \rightarrow D^{*+} \pi^- \pi^-$  (right) candidates.

TABLE 1. Branching fractions and resonance parameters for the  $D^{(*)+} \pi^- \pi^-$  final states.

| Mode                                            | $\mathcal{B}(B^- \rightarrow D_X [D^{(*)+} \pi^-] \pi^-)$ ,<br>$10^{-4}$ | $M(D_X)$ ,<br>MeV              | $\Gamma(D_X)$ ,<br>MeV           |
|-------------------------------------------------|--------------------------------------------------------------------------|--------------------------------|----------------------------------|
| $B^- \rightarrow D_2^{*0} [D^+ \pi^-] \pi^-$    | $3.4 \pm 0.3 \pm 0.6 \pm 0.4$                                            | $2462 \pm 2.1 \pm 0.5 \pm 3.3$ | $45.6 \pm 4.4 \pm 6.5 \pm 1.6$   |
| $B^- \rightarrow D_0^{*0} [D^+ \pi^-] \pi^-$    | $6.1 \pm 0.6 \pm 0.9 \pm 1.6$                                            | $2308 \pm 17 \pm 15 \pm 28$    | $276 \pm 21 \pm 18 \pm 60$       |
| $B^- \rightarrow D_1^0 [D^{*+} \pi^-] \pi^-$    | $6.8 \pm 0.7 \pm 1.3 \pm 0.3$                                            | $2421 \pm 1.5 \pm 0.4 \pm 0.8$ | $23.7 \pm 2.7 \pm 0.2 \pm 4.0$   |
| $B^- \rightarrow D_2^{*0} [D^{*+} \pi^-] \pi^-$ | $1.8 \pm 0.3 \pm 0.3 \pm 0.2$                                            | [5]                            | [5]                              |
| $B^- \rightarrow D_1^0 [D^{*+} \pi^-] \pi^-$    | $5.0 \pm 0.4 \pm 1.0 \pm 0.4$                                            | $2427 \pm 26 \pm 20 \pm 15$    | $384^{+107}_{-75} \pm 24 \pm 70$ |

presented in Table 1.

For the  $D^{*+} \pi^- \pi^-$  final state the fit of the density distribution is performed in four dimensional phase space to take into account the angles of the pion from  $D^*$  decay. The fit function includes both known  $D_2^{*0}$ ,  $D_1^0$  intermediate state contributions and a broad  $D^{*+} \pi^-$  resonance with free parameters. Figure 2(b) shows the  $D^{*+} \pi^-$  invariant mass distribution as well as the resulting fit. Together with the narrow resonances a clear

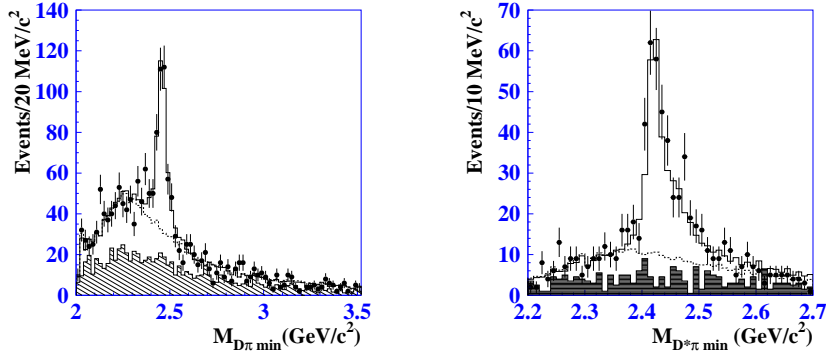


FIGURE 2. Minimal  $D^+ \pi^-$  (a) and  $D^{*+} \pi^-$  (b) invariant mass distributions. The points with error bars correspond to the  $B$  meson signal events, the hatched histogram shows the sidebands. The open histogram is the result of a fit while the dashed one shows the fit function without narrow resonance contribution.

signal of the broad state is observed. The angular distribution of  $D^*\pi$  from this state is consistent with  $J^P = 1^+$ ,  $j_q = 1/2$ . This state can be identified as a P-wave excitation of  $c\bar{u} - D_1^0$ . The results of the mass, width and branching fraction products are presented in Table 1.

Together with observations of the broad resonances the branching ratios of B decay to the modes with known  $D^{**}$ :  $D_1^0\pi^-$  and  $D_2^{*0}\pi^-$  have been measured. Using these measurements the ratio of  $D_2^{*0}$  branching fractions  $h = \mathcal{B}(D_2^{*0} \rightarrow D^+\pi^-)/\mathcal{B}(D_2^{*0} \rightarrow D^{*+}\pi^-) = 1.9 \pm 0.5$ , consistent with the world average  $h = 2.3 \pm 0.6$  [2], is obtained. The measured ratio  $R = \mathcal{B}(B^- \rightarrow D_2^{*0}\pi^-)/\mathcal{B}(B^- \rightarrow D_1^0\pi^-) = 0.77 \pm 0.15$  is lower than the CLEO measurement  $1.8 \pm 0.8$  [4] (although the results are consistent within errors) but is still a factor of two larger than the factorization prediction [6]. From our measurement it is impossible to determine whether the non-factorized part for tensor and axial mesons is large, or whether higher order corrections to the leading factorized terms should be taken into account.

Our measurements show that the narrow resonances compose  $(36 \pm 6)\%$  of the  $D\pi\pi$  decays and  $(63 \pm 6)\%$  of the  $D^*\pi\pi$  decays. This result is inconsistent with the QCD sum rule prediction and may indicate a large contribution from a color suppressed amplitude.

## OBSERVATION OF NEW STATES $D_{sJ}^+(2317)$ AND $D_{sJ}^+(2457)$

The narrow  $D_s\pi^0$  resonance at 2317 MeV, recently observed by the BaBar collaboration [7], is naturally interpreted as a P-wave excitation of the  $c\bar{s}$  system. The observation of a nearby and narrow  $D_s^*\pi^0$  resonance by the CLEO collaboration [8] supports this view, since the mass difference of the two observed states is consistent with the expected hyperfine splitting for a P-wave doublet with total light-quark angular momentum  $j = 1/2$  [9, 10]. The observed masses are, however, considerably lower than potential model predictions [11], and similar to those of the  $c\bar{u}$   $j = 1/2$  doublet states recently reported by Belle [3]. Measurements of the  $D_{sJ}$  quantum numbers and branching fractions (particularly those for radiative decays), will play an important role in determining the nature of these states.

We confirmed both resonances and measured masses for  $0^+$  and  $1^+$  states to be  $(2317.2 \pm 0.5 \pm 0.9)$  MeV and  $(2456.5 \pm 1.3 \pm 1.3)$  MeV respectively [12]. We also report the first observation of the radiative decay  $D_{sJ}(2457) \rightarrow D_s\gamma$ . Figure 3 shows the mass difference between the  $D_s^{(*)}\pi^0$  and  $D_s^{(*)}$  candidates. The ratio  $\frac{\mathcal{B}(D_{sJ}(2457) \rightarrow D_s\gamma)}{\mathcal{B}(D_{sJ}(2457) \rightarrow D_s^*\pi^0)}$  is found to be  $0.55 \pm 0.13 \pm 0.08$ .

We also search for  $D_{sJ}$  production in  $B \rightarrow DD_{sJ}$  decays [13]. We reconstruct  $\bar{D}^0(D^-)$  mesons in the  $K^+\pi^-$ ,  $K^+\pi^-\pi^-\pi^+$  and  $K^+\pi^-\pi^0$  ( $K^+\pi^-\pi^-$ ) decay channels.  $D_s^+$  mesons are reconstructed in the  $\phi\pi^+$ ,  $\bar{K}^{*0}K^+$  and  $K_S^0K^+$  decay channels.  $D_{sJ}$  candidates are reconstructed from  $D_s^{(*)}$  mesons and a  $\pi^0$ ,  $\gamma$ , or  $\pi^+\pi^-$  pair. The mass difference  $M(D_{sJ}) - M(D_s^{(*)})$  is used to select  $D_{sJ}$  candidates. We use central mass values of 2317 MeV and 2460 MeV for  $D_{sJ}(2317)$  and  $D_{sJ}(2457)$  respectively and define signal regions within 12 MeV for the corresponding mass difference. We observe a clean signal for  $B \rightarrow DD_{sJ}(2317)[D_s\pi^0]$  and  $B \rightarrow DD_{sJ}(2457)[D_s^*\pi^0]$ . We also observe for the first

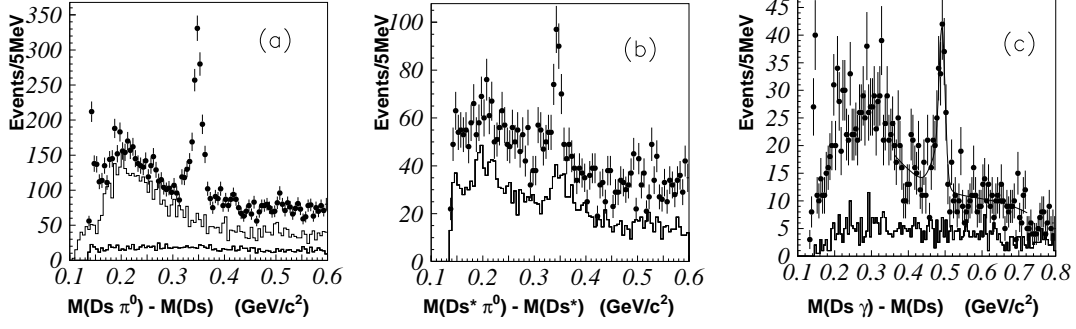


**FIGURE 3.**  $M(D_s \pi^0) - M_{D_s}$  (a),  $M(D_s^* \pi^0) - M_{D_s^*}$  (b) and  $M(D_s \gamma) - M_{D_s}$  (c) mass-difference distributions. The signal is described using a double Gaussian and a third-order polynomial for the background. The histogram shows no structure for the  $D_s^{(*)+}$  sidebands.

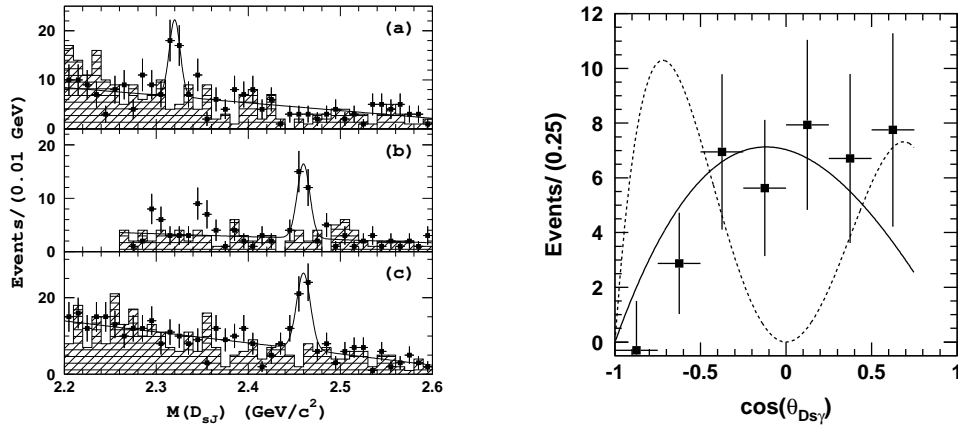


**FIGURE 4.** Left:  $M(D_{sJ})$  distribution for the  $B \rightarrow \bar{D} D_{sJ}$  candidates: (a)  $D_{sJ}(2317) \rightarrow D_s \pi^0$ , (b)  $D_{sJ}(2457) \rightarrow D_s^* \pi^0$  and (c)  $D_{sJ}(2457) \rightarrow D_s \gamma$ . Right: the  $D_{sJ}(2457) \rightarrow D_s \gamma$  helicity distribution. Points with errors represent the experimental data and curves are the results of the fits.

time the  $D_{sJ}(2457) \rightarrow D_s \gamma$  decay. Figure 4(left) shows the invariant mass distributions for these decays. The measured branching fractions are presented in Table 2. We obtain the ratio  $\frac{\mathcal{B}(D_{sJ}(2457) \rightarrow D_s \gamma)}{\mathcal{B}(D_{sJ}(2457) \rightarrow D_s^* \pi^0)} = 0.38 \pm 0.11 \pm 0.04$ , which is consistent with that from the continuum study.

We also study the helicity distribution for the  $D_{sJ}(2457) \rightarrow D_s \gamma$  decay. The helicity angle  $\theta_{D_s \gamma}$  is defined as the angle between the  $D_{sJ}(2457)$  momentum in the  $B$  meson rest frame and the  $D_s$  momentum in the  $D_{sJ}(2457)$  rest frame. The  $\theta_{D_s \gamma}$  distribution in the data (Fig. 4(right)) is consistent with MC expectations for the  $J = 1$  hypothesis for the  $D_{sJ}(2457)$  ( $\chi^2/\text{n.d.f.} = 5/6$ ), and contradicts the  $J = 2$  hypothesis ( $\chi^2/\text{n.d.f.} = 44/6$ ). The  $J = 0$  hypothesis is already ruled out by the conservation of angular momentum and parity in  $D_{sJ}(2457) \rightarrow D_s \gamma$ .

**TABLE 2.**  $B \rightarrow DD_{sJ}$  branching fractions.

| Decay channel                                       | $\mathcal{B}, 10^{-4}$       | Signif.     |
|-----------------------------------------------------|------------------------------|-------------|
| $B \rightarrow \bar{D}D_{sJ}(2317) [D_s\pi^0]$      | $8.5^{+2.1}_{-1.9} \pm 2.6$  | $6.1\sigma$ |
| $B \rightarrow \bar{D}D_{sJ}(2317) [D_s^*\gamma]$   | $2.5^{+2.0}_{-1.8} (< 7.5)$  | $1.8\sigma$ |
| $B \rightarrow \bar{D}D_{sJ}(2457) [D_s^*\pi^0]$    | $17.8^{+4.5}_{-3.9} \pm 5.3$ | $6.4\sigma$ |
| $B \rightarrow \bar{D}D_{sJ}(2457) [D_s\gamma]$     | $6.7^{+1.3}_{-1.2} \pm 2.0$  | $7.4\sigma$ |
| $B \rightarrow \bar{D}D_{sJ}(2457) [D_s^*\gamma]$   | $2.7^{+1.8}_{-1.5} (< 7.3)$  | $2.1\sigma$ |
| $B \rightarrow \bar{D}D_{sJ}(2457) [D_s\pi^+\pi^-]$ | $< 1.6$                      | —           |
| $B \rightarrow \bar{D}D_{sJ}(2457) [D_s\pi^0]$      | $< 1.8$                      | —           |

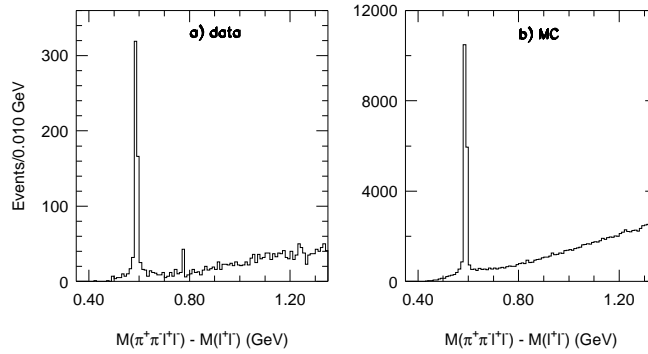


**FIGURE 5.** Distributions of  $M(\pi^+\pi^-l^+l^-) - M(l^+l^-)$  for selected events in the  $\Delta E$ - $M_{bc}$  signal region for (a) Belle data and (b) generic  $B\bar{B}$  MC events .

## OBSERVATION OF A NEW NARROW CHARMONIUM STATE IN $B^\pm \rightarrow K^\pm \pi^+ \pi^- J/\psi$ DECAY

A major experimental issue for the  $c\bar{c}$  charmonium particle system is the existence of as yet unestablished charmonium states that are expected to be below threshold for decays to open charm and, thus, narrow. These include the  $n = 1$  singlet P state, the  $h_c(1P)$ , and possibly the  $n = 1$  singlet and triplet spin-2 D states, i.e. the  $J^{PC} = 2^{-+} 1^1D_{c2}$  and  $J^{PC} = 2^{-+} 1^3D_{c2}$ , all of which are narrow if their masses are below the  $D\bar{D}^*$  threshold. The observation of these states and the determination of their masses would provide useful information about the spin dependence of the charmonium potential.

We report on an experimental study of the  $\pi^+\pi^-J/\psi$  and  $\gamma\chi_{c0}$  mass spectra from exclusive  $B^+ \rightarrow K^+\pi^+\pi^-J/\psi$  and  $K^+\gamma\chi_{c0}$  decays [15] using a 152M  $B\bar{B}$  event sample. For the  $B \rightarrow K\pi^+\pi^-J/\psi$  study we use events that have a pair of well identified oppositely charged electrons or muons with an invariant mass in the range  $3.077 < M_{l^+l^-} < 3.117$  GeV, a loosely identified charged kaon and a pair of oppositely charged pions.

Figure 5(a) shows the distribution of  $\Delta M \equiv M(\pi^+\pi^-l^+l^-) - M(l^+l^-)$  for events in the  $\Delta E$ - $M_{bc}$  signal region. Here a large peak corresponding to  $\psi(2S) \rightarrow \pi^+\pi^-J/\psi$  is evident at 0.589 GeV. In addition, there is a significant spike in the distribution at 0.775 GeV. Figure 5(b) shows the same distribution for a large sample of generic  $B\bar{B}$

**TABLE 3.** Results of the fits to the  $\psi(2S)$  and  $M = 3872$  MeV regions. The errors are statistical only.

| Quantity                                  | $\psi(2S)$ region    | $M = 3872$ MeV region |
|-------------------------------------------|----------------------|-----------------------|
| Signal events                             | $489 \pm 23$         | $35.7 \pm 6.8$        |
| $M_{\pi^+\pi^-J/\psi}^{\text{meas}}$ peak | $3685.5 \pm 0.2$ MeV | $3871.5 \pm 0.6$ MeV  |
| $\sigma_{M_{\pi^+\pi^-J/\psi}}$           | $3.3 \pm 0.2$ MeV    | $2.5 \pm 0.5$ MeV     |

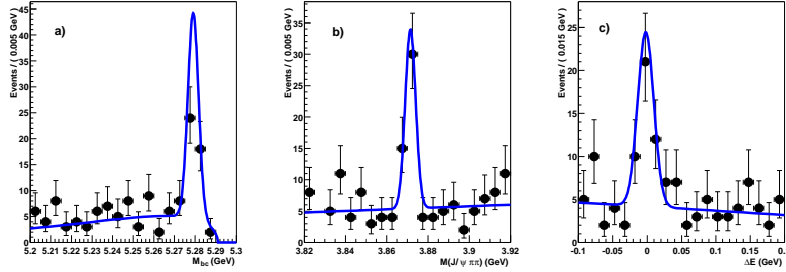


**FIGURE 6.** Signal-band projections of (a)  $M_{bc}$ , (b)  $M_{\pi^+\pi^-J/\psi}$  and (c)  $\Delta E$  for the  $X(3872) \rightarrow \pi^+\pi^-J/\psi$  signal region with the results of the unbinned fit superimposed.

Monte Carlo (MC) events. Except for the prominent  $\psi(2S)$  peak, the distribution is smooth and featureless.

We make separate fits to the data in the  $\psi(2S)$  ( $3580 \text{ MeV} < M_{\pi^+\pi^-J/\psi} < 3780 \text{ MeV}$ ) and the  $M = 3872$  MeV ( $3770 \text{ MeV} < M_{\pi^+\pi^-J/\psi} < 3970 \text{ MeV}$ ) regions using a simultaneous unbinned maximum likelihood fit to the  $M_{bc}$ ,  $\Delta E$ , and  $M_{\pi^+\pi^-J/\psi}$  distributions. The results of the fits are presented in Table 3. Figures 6(a), (b) and (c) show the  $M_{bc}$ ,  $M_{\pi^+\pi^-J/\psi}$ , and  $\Delta E$  signal-band projections for the  $M = 3872$  MeV signal region, respectively. The superimposed curves indicate the results of the fit. There are clear peaks with consistent yields in all three quantities. The signal yield of  $35.7 \pm 6.8$  events has a statistical significance of  $10.3\sigma$ . In the following we refer to this as the  $X(3872)$ .

We determine the mass of the signal peak relative to the well measured  $\psi(2S)$  mass:  $M_X = M_X^{\text{meas}} - M_{\psi(2S)}^{\text{meas}} + M_{\psi(2S)}^{\text{PDG}} = 3872.0 \pm 0.6 \pm 0.5 \text{ MeV}$ . Since we use the precisely known value of the  $\psi(2S)$  mass [2] as a reference, the systematic error is small. The measured width of the  $X(3872)$  peak is  $\sigma = 2.5 \pm 0.5 \text{ MeV}$ , which is consistent with the MC-determined resolution and the value obtained from the fit to the  $\psi(2S)$  signal. From this we infer a 90% confidence level (CL) upper limit of  $\Gamma < 2.3 \text{ MeV}$ .

We determine a ratio of product branching fractions for  $B^+ \rightarrow K^+ X(3872) [\pi^+\pi^-J/\psi]$  and  $B^+ \rightarrow K^+ \psi(2S) [\pi^+\pi^-J/\psi]$  to be  $0.063 \pm 0.012 \pm 0.007$ .

The decay of the  $^3D_{c2}$  charmonium state to  $\gamma\chi_{c0}$  is an allowed  $E1$  transition with a partial width that is expected to be substantially larger than that for the  $\pi^+\pi^-J/\psi$  final state; e.g. the authors of Ref. [16] predict  $\Gamma(^3D_{c2} \rightarrow \gamma\chi_{c0}) > 5 \times \Gamma(^3D_{c2} \rightarrow \pi^+\pi^-J/\psi)$ . Thus, a measurement of the width for this decay channel can provide important information about the nature of the observed state. We searched for an  $X(3872)$  signal in the  $\gamma\chi_{c0}$  decay channel, concentrating on the  $\chi_{c0} \rightarrow \gamma J/\psi$  final state.

We select events with the same  $J/\psi \rightarrow l^+l^-$  and charged kaon requirements plus two photons, each with energy more than 40 MeV. The signal-band projections of  $M_{bc}$

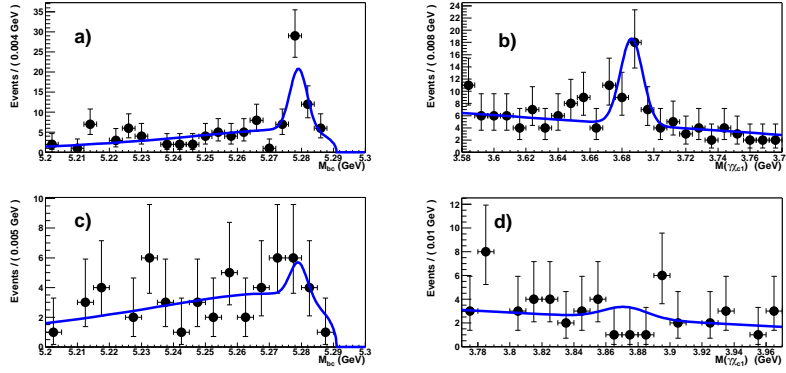


**FIGURE 7.** Signal-band projections of (a)  $M_{bc}$  and (b)  $M_{\gamma\chi_{c0}}$  for the  $\psi(2S)$  region with the results of the unbinned fit superimposed. (c) and (d) are the corresponding results for the  $M = 3872$  MeV region.

and  $M_{\gamma\chi_{c0}}$  for the  $\psi(2S)$  region are shown in Figs. 7 (a) and (b), respectively, together with curves that represent the results of the fit. The fitted signal yield is  $34.1 \pm 6.9 \pm 4.1$  events. The number of observed events is consistent with the expected yield of  $26 \pm 4$  events based on the known  $B \rightarrow K\psi(2S)$  and  $\psi(2S) \rightarrow \gamma\chi_{c0}$  branching fractions [2] and the MC-determined acceptance.

The results of the application of the same procedure to the  $M = 3872$  MeV region are shown in Figs. 7(c) and (d). Here, no signal is evident; the fitted signal yield is  $3.7 \pm 3.7 \pm 2.2$ . From these results, we determine a 90% CL upper limit on the ratio of partial widths of  $\frac{\Gamma(X(3872) \rightarrow \gamma\chi_{c0})}{\Gamma(X(3872) \rightarrow \pi^+\pi^-J/\psi)} < 0.89$ . This limit on the  $\gamma\chi_{c0}$  decay width contradicts expectations for the  $^3D_{c2}$  charmonium state.

The mass of the observed state is higher than potential model expectations for the center-of-gravity (cog) of the  $1^3D_{cJ}$  states:  $M_{\text{cog}}(1D) = 3810$  MeV [19, 18].

In summary, we have observed a strong signal for a state that decays to  $\pi^+\pi^-J/\psi$  with  $M = 3872.0 \pm 0.6 \pm 0.5$  MeV and  $\Gamma < 2.3$  MeV (90% CL). This mass value and the absence of a strong signal in the  $\gamma\chi_{c0}$  decay channel are in some disagreement with potential model expectations for the  $^3D_{c2}$  charmonium state. The mass is within errors of the  $D^0\bar{D}^{*0}$  mass threshold ( $3871.3 \pm 1.0$  MeV [2]), which is suggestive of a loosely bound  $D\bar{D}^*$  multiquark “molecular state,” as proposed by some authors [17].

## MEASUREMENT OF THE $E^+E^- \rightarrow D^{(*)+}D^{(*)-}$ CROSS-SECTIONS

The processes  $e^+e^- \rightarrow D^{(*)+}D^{(*)-}$  have not previously been observed at energies  $\sqrt{s} \gg 2M_D$ . A calculation in the HQET approach based on the heavy-quark spin symmetry [20], predicts cross-sections of about  $5 \text{ pb}^{-1}$  for  $e^+e^- \rightarrow D\bar{D}^*$  and  $e^+e^- \rightarrow D_T^*\bar{D}_L^*$  at  $\sqrt{s} \sim 10.6$  GeV (the subscripts indicate transverse [T] and longitudinal [L] polarization of the  $D^*$ ); the cross-section for  $e^+e^- \rightarrow D\bar{D}$  is expected to be suppressed by a factor of  $\sim 10^{-3}$ .

This analysis [21] is based on  $88.9 \text{ fb}^{-1}$  of data taken at or near the  $Y(4S)$  resonance. We reconstruct  $D^0$  and  $D^+$  mesons in the decay modes  $D^0 \rightarrow K^-\pi^+$ ,  $D^0 \rightarrow K^-\pi^+\pi^+\pi^-$  and  $D^+ \rightarrow K^-\pi^+\pi^+$ .  $D^{*+}$  mesons are reconstructed in the  $D^0\pi^+$  decay mode.

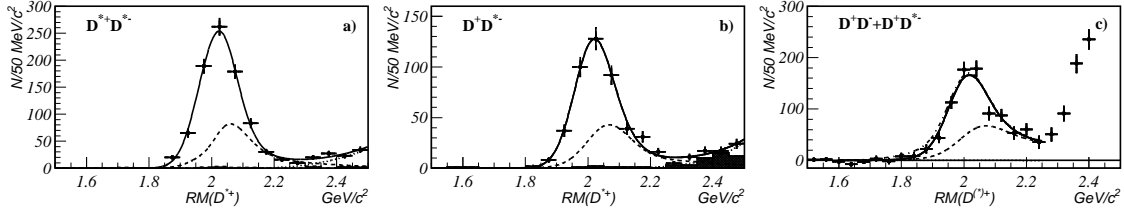


**FIGURE 8.** Distributions of the mass of the system recoiling against a)  $D^{*+}$ , and b)  $D^+$ . Points with error bars show the signal  $\Delta M_{\text{recoil}}$  region; hatched histograms correspond to  $\Delta M_{\text{recoil}}$  sidebands. The solid lines represent the fits described in the text; the dashed lines show the contribution due to events with ISR photons of significant energy. The dotted lines show the expected background contribution. c) The distribution of  $M_{\text{recoil}}(D^+)$  without any requirement on  $\Delta M_{\text{recoil}}$ .

The processes  $e^+e^- \rightarrow D^{(*)+}D^{(*)-}$  can be identified by energy-momentum balance in fully reconstructed events that contain only a pair of charm mesons. However, the reconstruction efficiency is small in this case. Taking into account two body kinematics, it is sufficient to reconstruct only one of the two charmed mesons in the event to identify the processes of interest. We choose the mass of the system recoiling against the reconstructed  $D^{(*)}$  ( $M_{\text{recoil}}(D^{(*)+})$ ) as a discriminating variable:  $M_{\text{recoil}}(D^{(*)+}) = \sqrt{(\sqrt{s} - E_{D^{(*)+}})^2 - \vec{p}_{D^{(*)+}}^2}$ , where  $E_{D^{(*)+}}$  and  $\vec{p}_{D^{(*)+}}$  are the CM energy and momentum of the reconstructed  $D^{(*)+}$ . For the signal a peak in the  $M_{\text{recoil}}$  distribution around the nominal mass of the recoiling  $D^-$  or  $D^{*-}$  is expected. This method provides a significantly higher efficiency, but also a higher background, in comparison to full event reconstruction. For the  $e^+e^- \rightarrow D^{(*)+}D^{*-}$  processes we reconstruct in addition a slow pion from the  $D^{*-} \rightarrow \bar{D}^0\pi_{\text{slow}}^-$  decay. This reduces the background to a negligible level.

We calculate the difference between the masses of the systems recoil mass against a  $D^{(*)+}\pi_{\text{slow}}^-$  combination, and against the  $D^{(*)+}$  alone,  $\Delta M_{\text{recoil}} \equiv M_{\text{recoil}}(D^{(*)+} - M_{\text{recoil}}(D^{(*)+}\pi_{\text{slow}}^-))$ . The variable  $\Delta M_{\text{recoil}}$  peaks around the nominal  $D^{*+} - D^0$  mass difference with a resolution of  $\sigma_{\Delta M_{\text{recoil}}} \sim 1$  MeV as found by Monte Carlo simulation. For  $e^+e^- \rightarrow D^{(*)+}D^{*-}$  we combine  $D^{(*)+}$  candidates together with  $\pi_{\text{slow}}^-$  and require  $\Delta M_{\text{recoil}}$  to be within a  $\pm 2$  MeV interval around the nominal  $D^{*+} - D^0$  mass difference.

The  $M_{\text{recoil}}(D^{*+})$  and  $M_{\text{recoil}}(D^+)$  distributions are shown in Figs. 8(a) and 8(b), respectively. Clear signals are observed in both cases. The higher recoil mass tails in the signal distribution are due to initial state radiation (ISR). The hatched histograms show the  $M_{\text{recoil}}$  distributions for events in the  $\Delta M_{\text{recoil}}$  sidebands.

Since the reconstruction efficiency depends on the production and  $D^{*\pm}$  helicity angles, we perform angular analysis before computing cross-sections. A scatter plot of the helicity angles for the two  $D^*$ -mesons from  $e^+e^- \rightarrow D^{*+}D^{*-}$  ( $\cos\phi(D_{\text{rec}}^*)$  vs  $\cos\phi(D_{\text{non-rec}}^*)$ ) for the recoil mass region  $M_{\text{recoil}}(D^{*+}) < 2.1$  GeV is shown in Fig. 9(a). The distribution is fitted by a sum of three functions corresponding to the  $D_T^*D_T^*$ ,  $D_T^*D_L^*$  and  $D_L^*D_L^*$  final states, obtained from Monte Carlo simulation. The fit finds the fractions of  $D_T^*D_T^*$ ,  $D_T^*D_L^*$  and  $D_L^*D_L^*$  final states to be  $(1.5 \pm 3.6)\%$ ,  $(97.2 \pm 4.8)\%$  and  $(1.3 \pm 4.7)\%$ , respectively. Figure 9(b) shows the  $D^{*-}$  meson helicity distribution for  $e^+e^- \rightarrow D^+D^{*-}$ . The fraction of the  $D^+D_L^{*-}$  final state is found from the fit to be equal



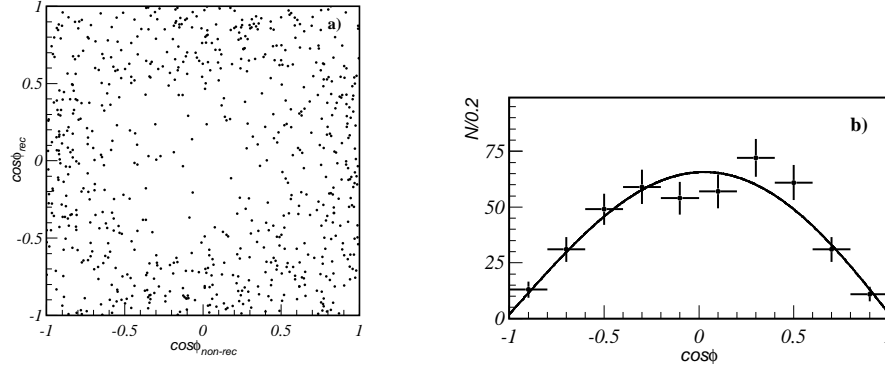


**FIGURE 9.** a) The scatter plot  $\cos(\phi_{D_{rec}^*})$  vs  $\cos(\phi_{D_{non-rec}^*})$  ( $e^+e^- \rightarrow D^{*+}D^{*-}$ ). b)  $D^{*+}$  meson helicity angle distribution for ( $e^+e^- \rightarrow D^+D^{*-}$ ) signal candidates.

to  $(95.8 \pm 5.6)\%$ .

We search for the process  $e^+e^- \rightarrow D^+D^-$  by studying the recoiling against the reconstructed  $D^+$  ( $M_{recoil}$ ). Fig. 8(c) shows the distribution of  $M_{recoil}(D^+)$  after  $D^+$  mass sideband subtraction. To extract the  $e^+e^- \rightarrow D^+D^-$  and  $e^+e^- \rightarrow D^+D^{*-}$  yields we fit this distribution with the sum of two signal functions corresponding to  $D^-$  and  $D^{*-}$  peaks and a threshold function describing background events. The fit finds  $-13 \pm 24$  events in the  $D^-$  peak and  $935 \pm 42$  in the  $D^{*-}$  peak. We obtain a  $e^+e^- \rightarrow D^+D^{*-}$  cross-section of  $0.61 \pm 0.05$  pb which agrees with the result using the  $\Delta M_{recoil}$  method. For the  $e^+e^- \rightarrow D^+D^-$  cross-section we set an upper limit of 0.04 pb at the 90% confidence level.

In summary, we report the first measurement of the cross-sections for the  $e^+e^- \rightarrow D^{*+}D^{*-}$  and  $e^+e^- \rightarrow D^+D^{*-}$  processes at  $\sqrt{s} = 10.6$  GeV to be  $0.65 \pm 0.04 \pm 0.07$  pb and  $0.71 \pm 0.05 \pm 0.09$  pb, respectively, and set an upper limit on the  $e^+e^- \rightarrow D^+D^-$  cross-section of 0.04 pb at 90% CL. The measured cross-sections are an order of magnitude lower than those predicted in Ref. [20], but their relative sizes are as predicted: the cross-sections for  $e^+e^- \rightarrow D^{*+}D^{*-}$  and  $e^+e^- \rightarrow D^+D^{*-}$  are found to be close each other, while the cross-section for  $e^+e^- \rightarrow D^+D^-$  is much smaller. The helicity decomposition for  $e^+e^- \rightarrow D^{*+}D^{*-}$  is found to be saturated by the  $D_T^{*\pm}D_L^{*\mp}$  final state (the fraction is equal to  $(97.2 \pm 4.8)\%$ ) and for  $e^+e^- \rightarrow D^+D^{*-}$  — by the  $D_L^*$  final state  $(95.8 \pm 5.6\%)$ , in good agreement with the predictions of Ref. [20].

## OBSERVATION OF $\eta_c(2S)$ PRODUCTION AND ITS MASS MEASUREMENT

Belle recently observed the  $\eta_c(2S)$  production in exclusive  $B$  decays to  $KKK_S^0\pi$ , where the  $\eta_c(2S)$  is reconstructed in the  $K^\pm K_S^0 \pi^\mp$  final state. The mass was measured to be  $(3654 \pm 6 \pm 8)$  MeV [22] which is much larger than the previous Crystal Ball measurement of  $(3594 \pm 5)$  MeV [23]. This year Belle also observed  $\eta_c(2S)$  production  $(108 \pm 24)$  events in double charmonia events  $e^+e^- \rightarrow J/\psi \eta_c(2S)$  and confirmed a

higher  $\eta_c(2S)$  mass [24].

## CONCLUSION

We have observed a strong signal for a new charmonium state that decays to  $\pi^+\pi^-J/\psi$  with  $M = 3872.0 \pm 0.6 \pm 0.5$  MeV,  $\Gamma < 2.3$  MeV at 90% CL. We confirm the observation of  $D_{sJ}(2317)$  and  $D_{sJ}(2457)$  and report the first observation of the decay  $D_{sJ}(2457) \rightarrow D_s\gamma$ . We also observe  $D_{sJ}$  production in  $B$  decays. In  $B^- \rightarrow D^{(*)+}\pi^-\pi^-$  decays all four P-wave  $D^{**}$  have been observed and their parameters have been measured. For the broad  $D_0^{*0}$  and  $D_1^{*0}$  states there are the first measurements.

## REFERENCES

1. Belle Collaboration, A. Abashian *et al.*, Nucl. Inst. and Meth. **A 479**, 117 (2002).
2. K. Hagiwara *et al.* (Particle Data Group), Phys. Rev. **D 66**, 010001 (2002).
3. Belle Collaboration, K.Abe, *et al.* hep-ex/0307021, submitted to Phys. Rev. D.
4. CLEO Collaboration, G. Gronberg *et al.*, CLEO CONF 96-25, Proc. of the ICHEP 96, July 1996, Poland.
5. Fixed from the  $D_2^{*0}$  parameters obtained in the  $B^- \rightarrow D^+\pi^-\pi^-$  analysis.
6. M. Neubert, Phys. Lett. **B 418**, 173 (1998).
7. BaBar Collaboration, B. Aubert *et al.*, Phys. Rev. Lett. **90**, (2003) 242001.
8. CLEO Collaboration, D. Besson *et al.*, hep-ex-0305017.
9. W. Bardeen, E Eichten and C. Hill, Phys. Rev. **D 68**, 054024 (2003).
10. In the heavy  $c$ -quark approximation, one expects two doublets of  $c\bar{s}$  states with quantum numbers  $J^P = 0^+, 1^+$  ( $j = 1/2$ ) and  $J^P = 1^+, 2^+$  ( $j = 3/2$ ). The second doublet has already been observed in  $DK$  and  $D^*K$  decays.
11. J. Bartelt and S. Shukla, Ann. Rev. Nucl. Part. Sci. **45** 133, (1995).
12. Belle Collaboration, Y.Mikami *et al.*, BELLE-CONF-0340, hep-ex/0307052, submitted to Phys. Rev. Lett.
13. Belle Collaboration, P.Krokovny *et al.*, hep-ex/0308019, submitted to Phys. Rev. Lett.
14. A. Palano for the BaBar Collaboration, hep-ex/0309028.
15. Belle Collaboration, S.-K.Choi, S.L.Olsen *et al.*, hep-ex/0309032, submitted to Phys. Rev. Lett.
16. E.J. Eichten, K. Lane, and C. Quigg, Phys. Rev. Lett. **89**, 162002 (2002). See also P. Ko, J. Lee and H.S. Song, Phys. Lett. **B395**, 107 (1997).
17. See, for example, M.B. Voloshin and L.B. Okun, JETP Lett. **23**, 333 (1976); A. De Rujula, H. Georgi and S.L. Glashow, Phys. Rev. Lett. **38**, 317 (1977); and N. Tornqvist, Z. Phys. **C 61**, 525 (1994).
18. E. Eichten, K. Gottfried, T. Kinoshita, K.D. Lane and T.M. Yan, Phys. Rev. **D 21**, 203 (1980).
19. W. Buchmüller and S-H.H. Tye, Phys. Rev. **D 24**, 132 (1981).
20. A. G. Grozin, M. Neubert, Phys. Rev. **D 55**, 272 (1997).
21. Belle Collaboration, K.Abe *et al.* BELLE-CONF-0332, hep-ex/0307084.
22. Belle Collaboration, S.-K.Choi, S.L.Olsen *et al.*, Phys. Rev. Lett. **89**, 102001 (2002)
23. Crystal Ball Collaboration, C.Edwards *et al.*, Phys. Rev. Lett. **48**, 70 (1982).
24. Belle Collaboration, K.Abe *et al.*, BELLE-CONF-0331.